Journal of Alloys and Compounds 504S (2010) S452–S455

Contents lists available at ScienceDirect

Journal of Alloys and Compounds

journal homepage: www.elsevier.com/locate/jallcom

Strain hardening behavior of nanostructured dual-phase steel processed by severe plastic deformation

Young Gun Ko[a,*], Chul Won Lee[b], Seung Namgung[b], Dong Hyuk Shin[b]

[a] School of Materials Science and Engineering, Yeungnam University, 214-1, Dae-Dong, Gyeongbuk, Gyeongsan 712-749, Republic of Korea
[b] Department of Metallurgy and Materials Science, Hanyang University, Ansan 425-791, Republic of Korea

ARTICLE INFO

Article history:
Received 3 July 2009
Received in revised form 11 January 2010
Accepted 10 February 2010
Available online 18 February 2010

Keywords:
Dual-phase steel
Nanostructure
Tensile properties
Strain hardening

ABSTRACT

The strain hardening behavior of nanostructured dual-phase steel fabricated by equal channel angular pressing together with subsequent intercritical annealing treatment was investigated. In contrast to conventional nanostructured steels that have negligible strain hardening capability in tension, the nanostructured dual-phase steel exhibited excellent strain hardenability due to the nanoscale grains of each constituent phase and their uniform distribution of them as well. The strain hardening behavior of such microstructure was explained by using modified Crussard–Jaoul analysis based on the Swift equation.

1. Introduction

In recent years, much attention has been paid to the development of metallic materials having nanostructured grains (below 1 μm), due to their superior mechanical properties, such as high strength, ductility, and even superplasticity at high strain rates [1–3]. Several techniques have been applied in conjunction with severe plastic deformation where the main deformation mode was the simple shear and, thereby, severe grain refinement could be readily attained through the continuous dynamic recrystallization [4,5]. Among these techniques, equal channel angular (ECA) pressing was regarded highly beneficial for tailoring a variety of nanostructured materials, depending on the deformation conditions, such as the number of pressings and fabrication routes. In steels, although samples with nanoscale grains exhibited their ultrahigh strength, at more than twice that of their coarse-grained counterparts, the inherent mechanical shortcoming of a lack of strain hardening capability, was unavoidable when they were deformed in tension. An earlier work attributed this unusual phenomenon to the dynamic recovery attained during tensile deformation and the size of the nanoscale grains being comparable to the mean free path of dislocations [6–8]. This limited strain hardening capability restricted the practical application of nanostructured materials. Thus, research attention has focused on overcoming this drawback by inducing nano-sized precipitates [9] and a bimodal grain size distribution [10] in the microstructure, but further investigation is required.

In the present study, a plain low-carbon steel was deformed by ECA pressing, and then was heat treated in the intercritical region ($\alpha+\gamma$) in order to fabricate a nanostructured dual-phase steel (DPS) having ferrite and martensite phases. DPS offer excellent formability at a similar strength to that of other high strength low-alloy steels. As it also has a low yield ratio and rapid strain hardening rate at the onset of plastic deformation, it was expected to overcome the typical shortcomings of nanostructured materials such as reduced strain hardenability and ductility [1,8]. Recently, Son et al. [11] fabricated the nanostructured DPS from the traditional, low-carbon steel consisting of ferrite and pearlite phases. Unfortunately, our repeated experiments suggested that their resultant microstructures were not uniform since the grain size of the ferrite phase (~30 μm) remained larger than the diffusion distance of carbon atoms during deformation. Accordingly, a martensitic structure was processed by ECA pressing and subsequently underwent intercritical annealing treatment followed by water quenching to control the uniform distribution of each constituent phase. The tensile properties were examined. Additionally, modified Crussard–Jaoul (C–J) analysis based on the Swift equation was conducted to explain the strain hardening behavior of the nanostructured DPS.

2. Experimental

The programmed material was a low-carbon steel plate with a chemical composition of 0.15%C–0.25%Si–1.1%Mn–Fe (in wt%). The thermo-mechanical treatment is shown in Fig. 1. First, the sample was austenitized at 1473 K for 1 h and then water-

* Corresponding author. Tel.: +82 53 810 2537; fax: +82 53 810 4628.
E-mail address: younggun@ynu.ac.kr (Y.G. Ko).

0925-8388/$ – see front matter © 2010 Elsevier B.V. All rights reserved.
doi:10.1016/j.jallcom.2010.02.109

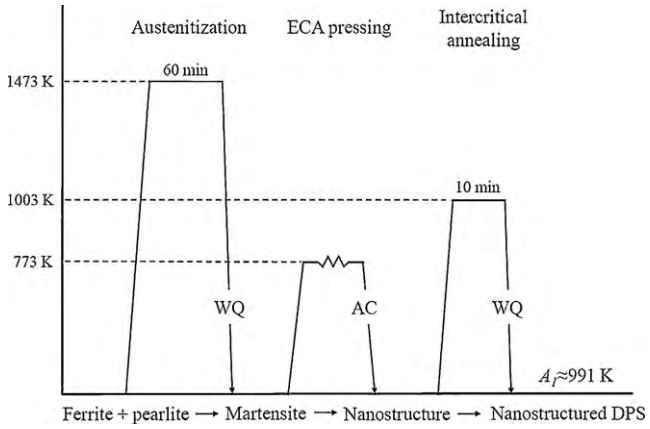

Fig. 1. Thermo-mechanical treatment to obtain the nanostructured DPS.

quenched, resulting in a fully martensitic structure with an average lath width of ~200 nm as shown in Fig. 2. After the sample was machined into a cylindrical specimen of 130 mm in length and 18 mm in diameter, four passes of ECA pressing (an effective strain of ~4) were carried out at 773 K with a route C method where the workpieces were consecutively rotated 180° along their longitudinal axis between each passage. The route C method is known to be effective in obtaining nearly equiaxed nanostructured grains, as an even number of passes ensures that the shear strain in the opposite direction is worked on by the same shear plane [12]. The deformed samples were heat treated at 1013 K for 10 min and water-quenched to fabricate a nanostructured DPS with a homogenous distribution of ferrite and martensite phases. For comparison, coarse-grained DPS was also prepared by the same intercritical annealing treatment.

The size and volume fraction of the ferrite and martensite phases were measured by scanning electron microscope (SEM, JEOL-6330F). The magnified structures were observed by transmission electron microscope (TEM, JEOL-2010). For TEM observation, thin foils were prepared by a twin-jet polishing technique using a mixture of 20% perchloric acid and 80% methanol at 233 K. The room-temperature tension tests were performed at a strain rate of $1.33 \times 10^{-3}\ s^{-1}$ on dog-bone specimens (gage length: 25.4 mm, and gage diameter: 6.25 mm) machined along the ECA pressing direction.

3. Results and discussion

3.1. Microstructural evolution

Fig. 3 displays the microstructural change of the steel sample prior to and following the intercritical annealing treatment after four-pass ECA pressing. Before the annealing treatment in the two-phase regime (Fig. 3a), the martensite packets were macroscopically deformed and bent throughout the microstructure. The deformed structure in Fig. 3b exhibited contain an ill-defined contrast and a high dislocation density in the vicinity of the (sub)grain boundaries, which was typical of several nanostructured materials that had undergone severe plastic deformation [1,2,10–14]. In addition, most of the grains were considerably refined to ~350 nm in diameter. After the intercritical annealing treatment, martensite phase grains appeared in an isolated blocky type. The equiaxed ferrite and blocky martensite phases with a grain size of ~1 μm were uniformly distributed and the volume fraction of the martensite phase was estimated to be ~35% (Fig. 4a). Like conventional DPS, a number of glissile dislocations, which were generated by transformation from austenite to martensite phases during cooling, were detected in the ferrite grains close to the martensite grains (Fig. 4b) [15]. This suggested that the nanostructured DPS here would exhibit moderate strain hardening behavior, in contrast to the previously reported nanostructured materials. As compared to the coarse-grained DPS (Fig. 1d in Ref. [13]), the nanostructured DPS exhibited significant differences in the morphological characteristics of the martensite such as the distribution, size, and shape. More importantly, carbon dissolution from the initial fully martensite phase would be easier during ECA pressing due to the strain-induced mechanical decomposition [16]. This phenomenon resulted in uniformly distributed austenite nucleation sites, and

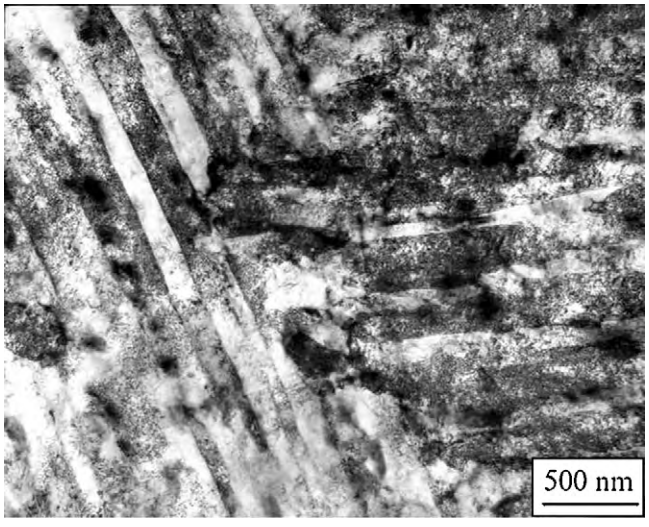

Fig. 2. Fully martensitic structure for ECA pressing and intercritical annealing treatment.

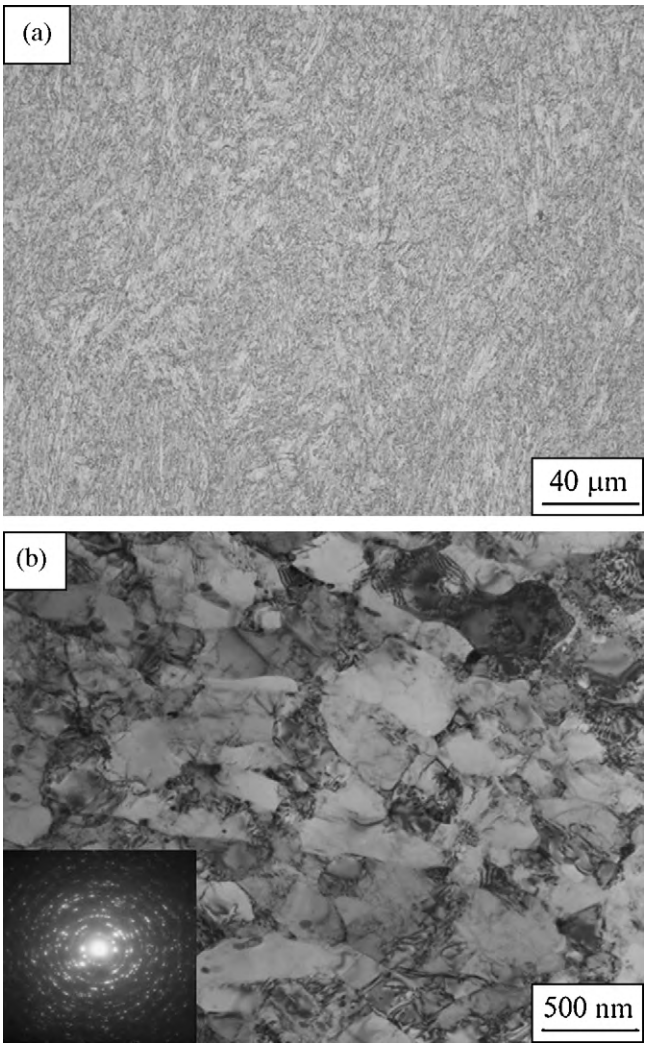

Fig. 3. (a) OM image and (b) TEM image of samples after deforming four-pass ECA pressing.

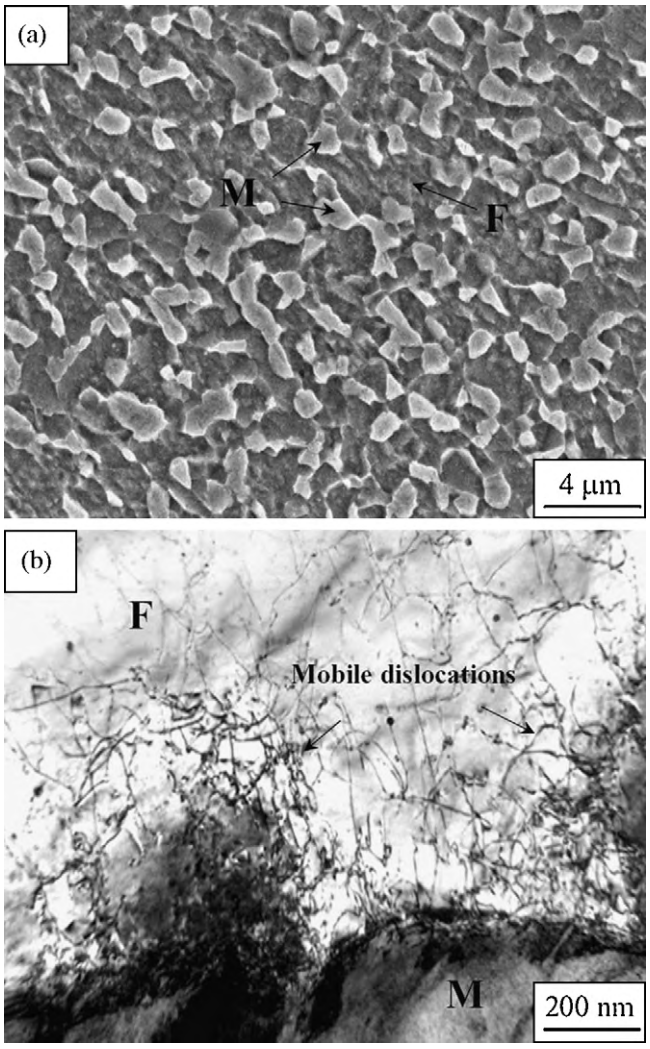

Fig. 4. (a) SEM image and (b) TEM image of the nanostructured DPS. F and M stand for the ferrite and martensite phases, respectively.

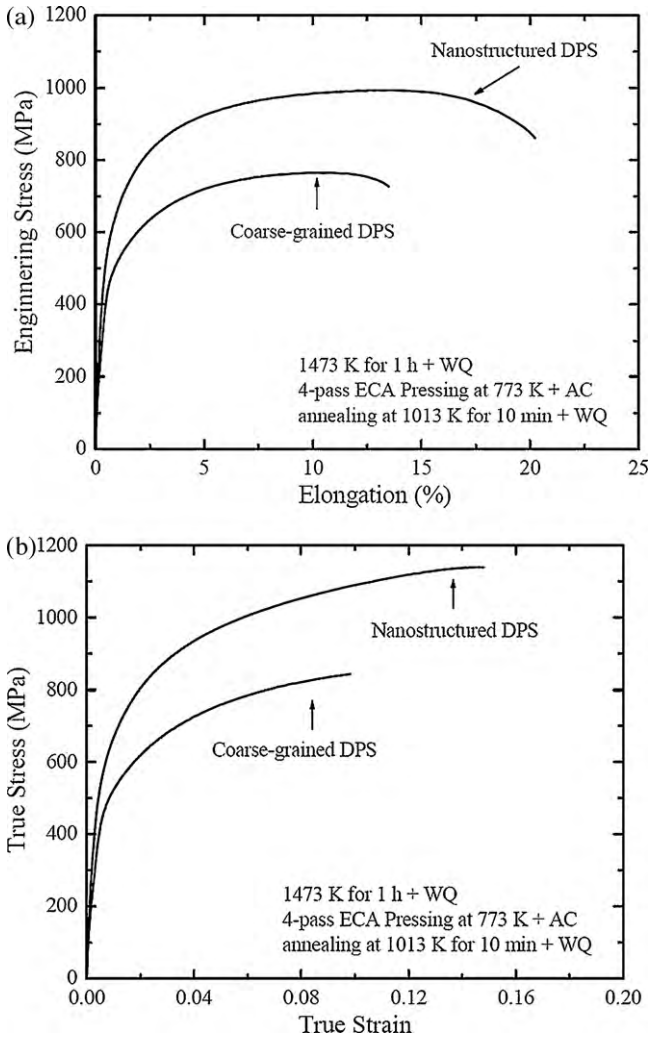

Fig. 5. (a) Engineering stress–strain curves and (b) true stress–strain curves of the nanostructured and coarse-grained DPSs.

inhibited the active grain growth of fine retained-ferrite during intercritical annealing at 733 K, thereby affording the present nanostructured DPS with a uniform distribution of each constituent phase.

3.2. Strain hardening behavior

The engineering and true stress–strain curves of the two different DPSs are shown in Fig. 5. The true stress–strain curves were plotted up to the uniform elongation determined by Considère's criterion for necking [17]. Two interesting findings were drawn. The apparent shape of the stress–strain curve in the nanostructured DPS was somewhat similar to that of its coarse-grained counterpart in that continuous yielding and rapid strain hardening occurred in the initial stage of plastic deformation. Hence, the two steels demonstrated the same yield ratio (~0.6), suggesting that the effect of grain size and volume fraction on the yield ratio was not appreciable. Second, the strength of the nanostructured DPS was significantly greater than that of coarse-grained one. In general, the strength of DPS is directly proportional to the volume fraction of the martensite phase [18], and dependent on the grain size of the ferrite phase according to the Hall–Petch relationship [19]. As a result, these two microstructural parameters induced the higher strength of the nanostructured DPS compared to that of the coarse-grained DPS.

As strain hardening capability is closely related to the ductility in tension, many investigations have analyzed the strain hardening by using various equations. The two empirical analyses based on classical equations have been commonly used: the Hollomon analysis based on the Hollomon equation [20] and the modified C–J analysis based on the Swift equation [21]. Those are as follows:

$$n_H = \frac{d(\ln \sigma)}{d(\ln \varepsilon)} \quad \text{Hollomon analysis} \tag{1}$$

$$\ln\left(\frac{d\sigma}{d\varepsilon}\right) = (1 - n_S)\ln\sigma - \ln(k_S n_S) \quad \text{modified C–J analysis} \tag{2}$$

in which σ and ε are the true stress and strain, respectively, and n_H and n_S are the strain hardening exponents that could be calculated by linear regression from the logarithmic plot of the iterated curves.

The two analyses were applied to the stress–strain data of the two DPSs in order to describe the strain hardening behavior. However, the application of the Hollomon equation only provided a monotonous relation, indicating that such analysis was unlikely to elucidate the strain hardening behavior of the DPS due to the variation in all microstructural parameters such as the size, distribution, and volume fraction of the ferrite and martensite phases. In contrast, the modified C–J analysis (Fig. 6) was sensitive to the phases present in the microstructure and, thus, produced two values associated with the two stages whose slope gave the value of $(1 - n_S)$. Fig. 6 reveals three implications. First, as mentioned above, DPS

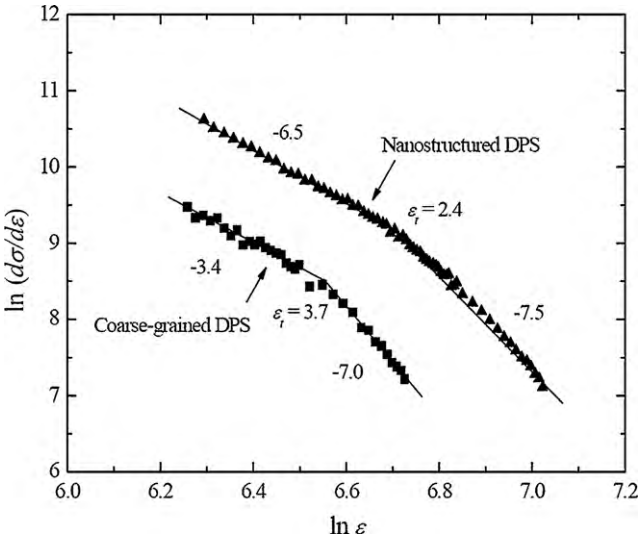

Fig. 6. A plot of $\ln(d\sigma/d\varepsilon)$–$\ln\sigma$ for the modified C–J analysis based on the Swift equation. The slope indicates $(1 - n_S)$.

normally exhibits two-stage hardening behavior after yielding has occurred. According to Jiang et al. [22], the ferrite phase is deformed plastically while the martensite phase remains elastic in the initial stage, whereas both phases are deformed plastically in the second stage. Second, the n_S value of the nanostructured DPS was higher than that of the coarse-grained DPS in the first stage. The higher n_S value of the nanostructured DPS in this stage was attributed to the fact that the plastic deformation of ferrite in the nanostructured DPS was more restrained by the martensite islands that had smaller interspacing compared to those of the coarse-grained DPS. However, the n_S values became comparable in the following stage. Plastic deformation was mainly governed by the martensite phase, so that nearly the same values were found in the second region. Third, the transition strain between the first and second stages was smaller in the nanostructured DPS (2.8%), than in the coarse-grained DPS (3.7%), indicating that the plastic deformation of martensite in the nanostructured DPS started earlier than that in the coarse-grained DPS. The higher n_S value of the nanostructured DPS in the first stage further reinforced this rationale.

4. Conclusions

By using a fully martensitic structure as the starting microstructure, DPS with a uniform distribution of nanostructured grains of ferrite and martensite phases was fabricated through ECA pressing followed by intercritical heat treatment and water quenching. Unlike several nanostructured steels, the present DPS showed a good combination of strength and ductility due to its excellent strain hardenability.

Acknowledgement

This work was supported by the Korea Research Foundation (KRF-2007-357-D00136) of the Korea Government.

References

[1] R.Z. Valiev, R.K. Islamgaliev, I.V. Alexandrov, Prog. Mater. Sci. 45 (2000) 103–189.
[2] R.Z. Valiev, Nat. Mater. 3 (2004) 511–516.
[3] Y.G. Kim, Y.G. Ko, D.H. Shin, C.S. Lee, S. Lee, J. Korean Inst. Met. Mater. 47 (2009) 397–405.
[4] Y.L. Choi, S.H. Kim, Met. Mater. Int. 14 (2008) 695–699.
[5] R.D. Doherty, D.A. Hughes, F.J. Humphreys, J.J. Jonas, D. Juul Jensen, M.E. Kassner, W.E. King, T.R. McNelley, H.J. McQueen, A.D. Rollett, Mater. Sci. Eng. A 238 (1997) 219–274.
[6] A.A. Nazarov, A.E. Romanov, R.Z. Valiev, Scr. Metall. 24 (1990) 1929–1934.
[7] H. Conrad, J. Narayan, Acta Mater. 50 (2002) 5067–5078.
[8] Y.G. Ko, D.H. Shin, K.-T. Park, C.S. Lee, Scr. Mater. 54 (2006) 1785–1789.
[9] C.C. Koch, Scr. Mater. 49 (2003) 657–662.
[10] R.Z. Valiev, Nature 419 (2002) 887–889.
[11] Y.I. Son, Y.K. Lee, K.-T. Park, C.S. Lee, D.H. Shin, Acta Mater. 53 (2005) 3125–3134.
[12] S. Komura, Z. Horita, M. Furukawa, M. Nemoto, T.G. Langdon, Metall. Mater. Trans. A 32 (2001) 707–716.
[13] K.-T. Park, S.Y. Han, B.D. Ahn, D.H. Shin, Y.K. Lee, K.K. Um, Scr. Mater. 51 (2004) 909–913.
[14] S.Z. Han, M. Goto, C. Lim, C.J. Kim, S. Kim, J. Alloys Compd. 434–435 (2007) 304–306.
[15] D.K. Matlock, F. Zia-Ebrahimi, G. Krauss, in: G. Krauss (Ed.), Deformation, Processing, and Structure, ASM, Metals Park, OH, 1982, pp. 47–83.
[16] D.A. Porter, K.E. Eastering, Phase Transformations in Metals and Alloys, second ed., Chapman and Hall, London, 1992, pp. 263–381.
[17] A. Considère, Ann. Ponts et Chaussées 9 (1885) 574–775.
[18] R.G. Davis, Metall. Trans. A 9 (1978) 671–679.
[19] N.J. Kim, G. Thomson, Metall. Trans. A 12 (1981) 483–489.
[20] J.H. Hollomon, Trans. Metall. Soc. AIME 162 (1945) 268–290.
[21] H.W. Swift, J. Mech. Phys. Solids 1 (1952) 1–18.
[22] Z. Jiang, Z. Guan, Z. Lian, Mater. Sci. Eng. A 190 (1995) 55–64.